Relaxor ferroelectric behavior in Ca-doped $TbMnO_3$

N. Mufti,[1] A. A. Nugroho,[1,2] G. R. Blake,[1] and T. T. M. Palstra[1]
[1]*Solid State Chemistry Laboratory, Zernike Institute for Advanced Materials, Rijksuniversiteit Groningen, Nijenborgh 4, 9747 AG Groningen, The Netherlands*
[2]*Faculty of Mathematics and Natural Sciences, Institut Teknologi Bandung, Jl. Ganesha 10, Bandung 40132, Indonesia*
(Received 14 May 2008; revised manuscript received 6 June 2008; published 11 July 2008)

We have studied the effect of Ca-doping in single-crystal $Tb_{1-x}Ca_xMnO_3$($x \leq 0.1$) on the crystal and magnetic structure, magnetocapacitance, and electric polarization. For low doping ($x=0.05$), the presence of Mn^{4+} ions gives rise to a state with behavior resembling that of a relaxor ferroelectric. The coherence length of the Mn magnetic spin spiral is reduced, while the Mn-modulation wave vector is unchanged. For doping larger than 5%, the ferroelectric state is suppressed, which we ascribe to breakdown of the spiral magnetic structure.

DOI: 10.1103/PhysRevB.78.024109 PACS number(s): 77.80.−e, 75.47.Lx, 77.84.−s

I. INTRODUCTION

The rare-earth manganites $RMnO_3$, with R=Gd, Tb, and Dy, exhibit a new type of ferroelectricity induced by a magnetic spiral structure.[1–5] They first develop incommensurate sinusoidal antiferromagnetic order below about 40 K. The incommensurability continuously changes upon cooling and becomes almost constant below the "lock-in" temperature $T_{lock} \simeq 28$ K and $\simeq 19$ K for R=Tb and Dy, respectively. For R=Gd, a sudden drop of the incommensurability vector is observed below $T_{lock} \simeq 23$ K.[2,6,7] The transition to this long-wavelength incommensurate antiferromagnetic phase for R=Tb and Dy is accompanied by ferroelectric ordering with a spontaneous electric polarization $P \| c$. The polarization flops to $P \| a$ when a magnetic field above a critical value is applied along the a or b direction, while it is suppressed for large fields applied along c. In contrast, for R=Gd, a polarization ($P \| a$) is only observed for magnetic fields greater than 1 T applied along the b axis.[3] Recently, the polarization has been reversed in $TbMnO_3$ by rotating the direction of the magnetic field in the ab plane; the $4f$ moment was found to play an important role in the polarization flop.[8] The origin of the ferroelectric state in $TbMnO_3$ is based on the existence of a spiral magnetic structure below T_{lock}, which breaks both time reversal and inversion symmetry. It has been described theoretically by microscopic[9] and Landau phenomenological models.[5] Both approaches show that the direction of the polarization is perpendicular to the spin rotation axis and the wave vector of the magnetic spiral. An associated lattice distortion with a doubled wave vector develops together with the Mn spiral. A recent structural investigation of $DyMnO_3$ has shown that a further lattice distortion develops below the Dy-spin ordering temperature; it originates from coupling between the rare-earth and Mn magnetic moments, which shows that the rare-earth sublattice should also be taken into account to understand the multiferroic properties.[10]

The effects of doping the rare-earth site with a divalent cation such as Ca, Sr, and Ba on the spin, charge, and orbital degrees of freedom in $RMnO_3$ have been extensively investigated. However, most studies have focused on large doping; in particular, the consequences of introducing charge carriers for the ferroelectric properties of $R_{1-x}A_xMnO_3$ for x less than 10% (R=Gd, Tb, Dy) have not yet been explored. Therefore, we have synthesized single crystals of $Tb_{1-x}Ca_xMnO_3$ with nominal x=0, 0.02, 0.05, and 0.1, and investigated their magnetic, structural, and electric properties. We find that both the ferroelectric ordering temperature and the magnitude of the spontaneous polarization are suppressed with increasing carrier concentration. Our data indicate that Ca doping destroys the ferroelectric state as well as the spiral magnetic structure via an intermediate state that resembles a relaxor ferroelectric. We present a magnetic-electric phase diagram for Ca-doped $TbMnO_3$ in terms of the perovskite tolerance factor.

II. EXPERIMENT

Single-crystalline samples of $Tb_{1-x}Ca_xMnO_3$ with nominal values of x=0, 0.02, 0.05, and 0.1 were grown by the floating zone method using a four-mirror furnace (Crystal Systems Inc., FZT-10000-H-VI-VP). To make the feed rod for crystal growth, stoichiometric amounts of Tb_4O_7, $CaCO_3$, and a 1% excess of MnO_2 were mixed, ground, calcined at 1000 °C, and sintered at 1200 °C in air for 36 h with intermediate grindings. The mixture was then compressed hydrostatically at 600 bar in a rubber tube into a rod of diameter 7 mm and length 50 mm. This rod was heated in air at 1400 °C for 12 h. The crystal-growth rate was between 1.5 and 5 mm/h and was carried out in air. The seed and feed rods were counter-rotated at a speed of 15–20 rpm. The crystallinity of the sample was checked by Laue diffraction and cut crystal pieces were oriented using an Enraf-Nonius CAD4 single-crystal diffractometer. Temperature dependent x-ray powder diffraction was performed on crushed single-crystal pieces using a Huber diffractometer equipped with a G670 Guinier camera and a closed-cycle refrigerator. The magnetic properties were measured using a Quantum Design MPMS-7 SQUID magnetometer. The dielectric constant was measured using an Agilent 4284A LCR meter in combination with a Quantum Design physical properties measurement system. For polarization measurements, the samples were cooled in a poling electric field of ~150 V/mm. After poling, the polarization was determined by integrating the pyroelectric current. Changing the sign of the poling field resulted in a change of sign of the pyroelectric current, proving the ferroelectric nature of our samples. Single-crystal

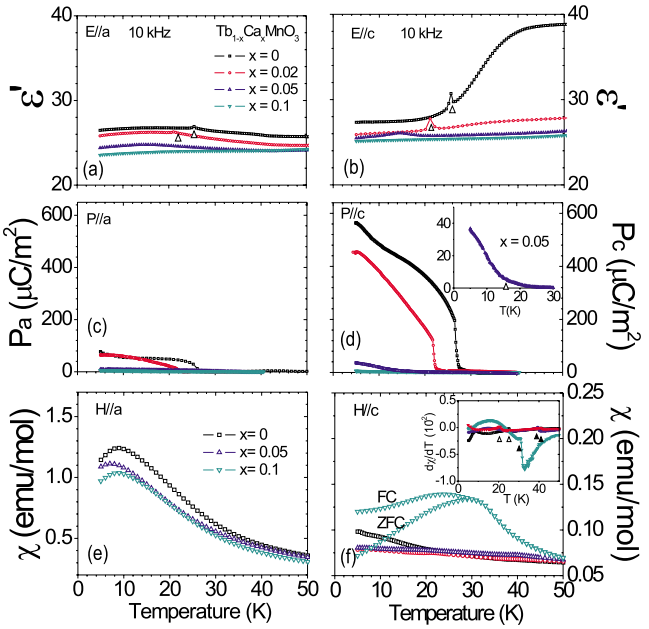

FIG. 1. (Color online) Temperature dependence of the dielectric constant of $Tb_{1-x}Ca_xMnO_3$ along the (a) *a* axis and (b) *c* axis; spontaneous polarization along the (c) *a* axis and (d) *c* axis; magnetic susceptibility measured on heating after cooling in zero field or in 0.5 T field applied along the (e) *a* axis and (f) *c* axis. In all panels (a) to (f) open and closed triangles indicate the antiferromagnetic ordering (T_N) and ferroelectric transition (T_{lock}) temperatures, respectively.

neutron-diffraction experiments were carried out at the Berlin Neutron Scattering Center (BENSC) using the double-axis E4 instrument. Single crystals of approximate size 5 $\times$5 mm were oriented with the *bc* plane in the scattering plane. Cooling was achieved using a standard orange cryostat.

III. RESULTS

Figure 1 shows the temperature dependence of the dielectric constant (ε), spontaneous polarization (P), and magnetic susceptibility (χ) of $Tb_{1-x}Ca_xMnO_3$ parallel to the *a* and *c* axes. Anomalies in $\varepsilon(T)$ are present at $T_{\text{lock}} \sim 26$ K and ~ 21 K for the $x=0$ and 0.02 samples, respectively. For $x=0.05$, the dielectric anomaly becomes broad and is observed at $T \sim 15$ K for $E \| c$. No dielectric anomaly appears for $x=0.1$ in either direction. A spontaneous polarization is observed for $x=0$ and $x=0.02$ for $P \| c$ and $P \| a$, as shown in Figs. 1(c) and 1(d). The small polarization $P \| a$ is most likely a result of slight crystal misalignment. The polarization of the $x=0$ and $x=0.02$ samples suddenly appears at T_C, typical of a ferroelectric transition. However, for $x=0.05$, the onset of the polarization appears to occur much more gradually, pointing to a phase transition of diffuse character. The magnetic susceptibility exhibits anomalies only for $H \| c$ [Fig. 1(f)], which correlate with the anomalies in $\varepsilon(T)$ and $P(T)$. However, the position of the broad peak in $\varepsilon(T)$ for $x=0.05$ is dependent on the measurement frequency. As shown in Fig. 2, the peak shifts to higher temperature as the frequency

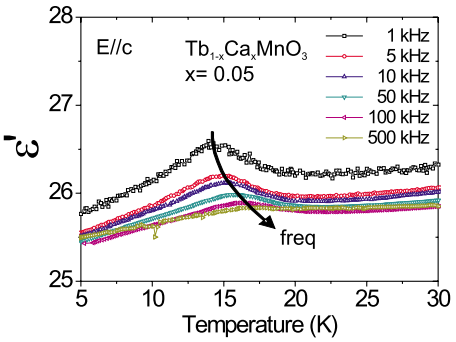

FIG. 2. (Color online) Temperature dependence of the dielectric constant of $Tb_{0.95}Ca_{0.05}MnO_3$ for different frequencies.

increases. The presence of a diffuse phase transition and a broad frequency-dependent peak in the real part of the temperature dependent dielectric susceptibility are both typical features of relaxor ferroelectrics.[11] The magnetization measurement for $x=0.1$ shows spin-glass-like behavior, which can be ascribed to the existence of ferromagnetic clusters. It is well known that the mixed-valent state containing Mn^{3+} and Mn^{4+} yields ferromagnetic interactions via the double-exchange (DE) mechanism. If the Mn^{4+} concentration is low, long-range ferromagnetic order is not achieved. Similar behavior was previously reported for $Tb_{0.85}Ca_{0.15}MnO_3$.[12]

To investigate the effect of Ca doping on the magnetic structure, we used neutron diffraction to study the temperature dependence of the Mn-spin modulation of $Tb_{1-x}Ca_xMnO_3$ with $x=0.02$ and $x=0.05$. So-called *A*-type magnetic superlattice reflections, characteristic of the Mn-spin modulation, were observed at $(0, 2-q, 1)$ and $(0, 2+q, 1)$ in both samples, but were much stronger for $x=0.02$ at all temperatures [see Fig. 3(a)]. Here, q is the Mn spin-spiral propagation vector parallel to the *b* axis. We normalized the integrated intensities of these superlattice reflections to the intensity of the main (002) reflection, which contains no magnetic component. The Mn spin modulation in both samples has the same periodicity as in undoped $TbMnO_3$, where $q \sim 0.28$. In Fig. 3(a) the temperature dependence of the intensity of the $(0, 2+q, 1)$ reflection is shown; the intensities were obtained from omega scans. It increases in intensity below $T_C \sim 21$ K and $T_C \sim 15$ K for $x=0.02$ and $x=0.05$, respectively. No superlattice reflections were observed above the magnetic ordering temperature of 42 K. This behavior is slightly different to that in undoped $TbMnO_3$,[7] where the increase in intensity of the *A*-type reflections in the vicinity of T_C is much less pronounced. Figure 3(b) shows the temperature dependence of the peak width of the $(0, 2+q, 1)$ reflection. It is clear that the *A*-type peaks for $x=0.05$ are broader than those for $x=0.02$ below T_C, indicating that increased Ca-doping decreases the coherence length of the Mn spin-spiral structure, leading to shorter-range order.

Figure 4 shows the temperature dependence of the lattice parameters of $Tb_{1-x}Ca_xMnO_3$ with $x=0$, 0.02, 0.05, and 0.1 obtained from x-ray powder diffraction on crushed single crystals. The diffraction patterns were consistent with space group *Pbnm* at all temperatures; although the lattice is known to become incommensurate below T_N,[3,4,13] no addi-

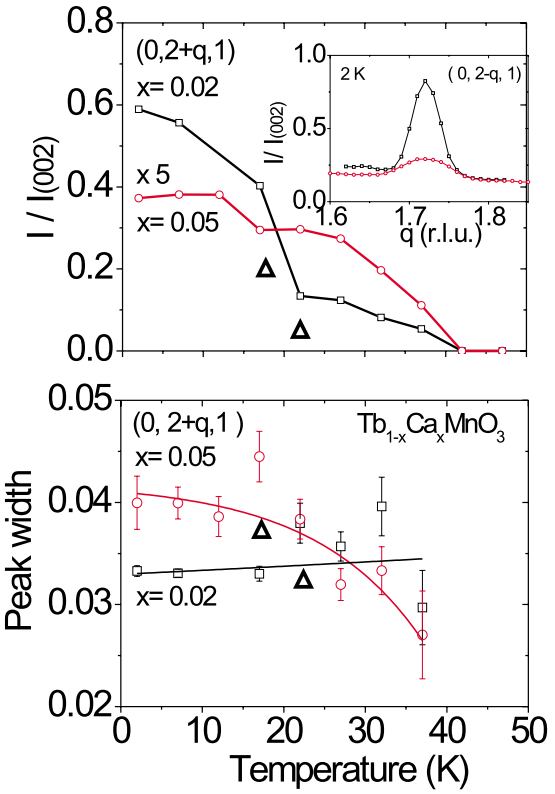

FIG. 3. (Color online) (a) Temperature dependence of normalized integrated intensity of the $(0, 2+q, 1)$ peak. The inset shows k scans around $(0, 2-q, 1)$ at 2 K. (b) Width of $(0, 2+q, 1)$ peak. The open triangles indicate the ferroelectric transition (T_{lock}) temperatures. The solid lines are guides to the eye.

tional satellite peaks were observed and thus the lattice parameters are those of the average structure. The a axis shows almost no dependence on doping below 50 K, whereas the c axis increases slightly with increasing Ca content. In contrast, the b lattice parameter rapidly decreases. $TbMnO_3$ has a strongly distorted orthorhombic structure due to the size mismatch between Tb^{3+} and Mn^{3+}, manifested by the large differences between the a and b lattice parameters. This type of distortion is also correlated with the magnitude of the Jahn-Teller distortion of Mn^{3+} in the MnO_6 octahedra.[12,13] With increasing Ca content, both the orthorhombic and octahedral distortion decrease, giving rise to a rapid decrease in the b-lattice parameter.[12] We also observe a distinct discontinuity in the lattice parameters of our $x=0$ sample at $T\sim 26$ K, which becomes continuous after doping. The temperature at which the discontinuity occurs coincides with the ferroelectric transition temperature. The largest discontinuity is along the c axis, which is the direction of the spontaneous polarization. These discontinuities are qualitatively comparable with the anomalies in the thermal expansion at T_{lock} reported by Meier *et al.*[14] This implies that there is strong coupling between the ferroelectricity and the lattice structure.

IV. DISCUSSION

For $RMnO_3$ perovskites, an increasing ionic radius of the rare-earth results in an increase of the Mn-O-Mn bond angle.[19] A similar effect is observed for Ca-doping on the A site when R is smaller than Ca; doping increases the Mn-O-Mn bond angles in the ab plane.[12,15] However, there is a marked difference: for Ca-doping, the valence change induced on the B site dominates the change of ionic radius of the A site.[16] For example, the difference in ionic radius between Mn^{4+}(0.53 Å) and Mn^{3+}(0.645 Å) is a greater factor in determining the structure than the difference between Ca^{2+}(1.18 Å) and Tb^{3+}(1.095 Å). Both effects are taken into account in the perovskite tolerance factor (t), which is linearly related to the average Mn-O-Mn bond angle (see the inset of Fig. 5).[17–19] The average Mn-O-Mn bond angles in Fig. 5 are taken from Refs. 13 and 17–19. In calculating t, we have used ionic radii from Ref. 20 and a coordination number of nine for the A site, because these values have been most accurately determined for small rare-earth ions. The amount of Mn^{4+} present on the B site was assumed to be the same as the Ca content.[12] As shown in Fig. 5, the effect of Ca doping in $Tb_{1-x}Ca_xMnO_3$ can be divided into two regimes. First, for $x\leq 0.05$, the effect of the tolerance factor or Mn-

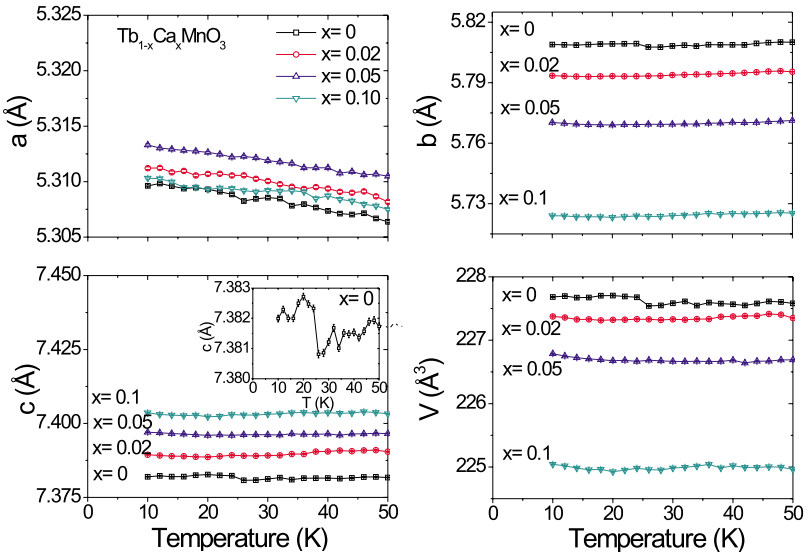

FIG. 4. (Color online) (a) Temperature dependence of the lattice parameters and volume of crushed single crystals of $Tb_{1-x}Ca_xMnO_3$. The inset shows the detailed thermal evolution of the c axis of $TbMnO_3$.

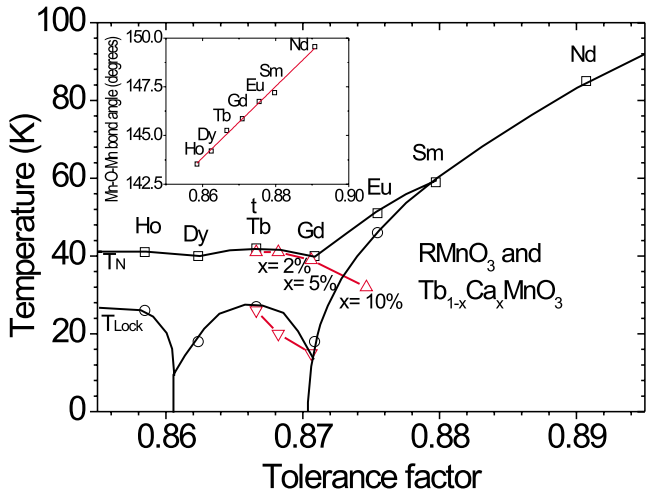

FIG. 5. (Color online) Phase diagram of $R\mathrm{MnO_3}$ and $\mathrm{Tb_{1-x}Ca_xMnO_3}$ with ordering temperatures as a function of tolerance factor. The inset shows a plot of the average Mn-O-Mn bond angle as a function of tolerance factor. Red triangles correspond to samples doped with $x=0$, 0.02, 0.05, and 0.1 of Ca.

O-Mn bond angle dominates. Doping causes a weakening of the relative strength of the next-nearest neighbor superexchange interactions.[13] This results in a partial breakdown of the spiral structure for $x=0.05$ and probably to increasing preference for the A-type antiferromagnetic structure at low temperature; this has previously been found in $\mathrm{GdMnO_3}$, which has the same tolerance factor. Second, for $0.05<x\leq 0.1$, the effect of double-exchange interactions becomes dominant, and the magnetic structure transforms to a spin-glass-like state. This behavior can be explained by the emergence of ferromagnetic clusters.[12]

The onset of polarization in our $x=0.05$ sample occurs in a rather diffuse fashion [Fig. 1(d)], suggesting that the ferroelectricity may be of the relaxor type. In order to clarify this issue, we measured the temperature dependence of the dielectric constant at different frequencies (see Fig. 2). The broad peak shifts with increasing frequency to higher temperature. This behavior resembles that of a relaxor ferroelectric, in which the maximum of the broad peak defines a glasslike transition temperature T_m associated with a diffuse phase transition where the dipolar fluctuations within small polar domains slow down. In relaxor ferroelectrics, these domains are paraelectric at high temperatures. Upon cooling they transform to polar nanoregions (PNR), each with a randomly oriented dipole moment. At sufficiently low temperatures all dipolar motion freezes, and the dispersion vanishes.[11] The existence of PNR in relaxor ferroelectrics is a universal feature, although the precise mechanism of their formation is still debated.[21] In conventional relaxor ferroelectrics, PNR are often generated from the disturbance of long-range order (LRO) by compositional disorder, impurities, lattice vacancies, or other imperfections. The correlation that PNR have with the magnetic structure is unclear because known relaxors are generally nonmagnetic. In contrast, the relaxor behavior of our $x=0.05$ sample occurs below the magnetic ordering temperature. As we show in Fig. 3, the Mn magnetic peak is broader for $x=0.05$ than for $x=0.02$. This implies that the relaxor behavior originates from a decreased coherence length of the Mn-spin-spiral structure. No similar mechanism has previously been reported, and therefore we propose that $\mathrm{Tb_{1-x}Ca_xMnO_3}$ might form a new class of relaxor ferroelectrics in which the relaxor behavior is induced by the magnetic structure. We note that further experimental evidence, such as can be obtained by neutron diffuse scattering, is needed to prove the existence of PNR in our materials.

Recently, theoretical calculations have shown that the direction of the polarization in $R\mathrm{MnO_3}$ depends on the helicity of the spiral mode, which is either clockwise or counterclockwise.[5,9] Thus, for our $x=0.05$ sample, where SRO spiral structures are randomly oriented, both spiral modes are likely to exist. In this scenario, the polarization of spiral domains with opposite handedness will cancel and the net polarization will decrease rapidly with doping. Alternatively, the spiral ordering might simply be disrupted by doping, eventually giving way to double exchange and leading to a decrease in the coherence length of the spiral, or to shorter-range order.

V. CONCLUSION

A small degree of Ca-doping suppresses the ferroelectric state in $\mathrm{Tb_{1-x}Ca_xMnO_3}$. This transition is governed by the appearance of $\mathrm{Mn^{4+}}$, which causes both the Mn-O-Mn bond angle and the influence of double-exchange interactions to increase. The suppression of ferroelectricity with doping occurs via an intermediate state at $x=0.05$ with behavior resembling that of a relaxor. The intermediate state is associated with a decreased coherence length of the Mn spin-spiral structure, without any change in the modulation wave vector. The ferroelectric transition is signaled by lattice discontinuities, where the largest lattice anomaly corresponds to the direction of the polarization.

ACKNOWLEDGMENTS

The authors are grateful to M. Mostovoy, D. Argyriou, and U. Adem for useful discussions, and to K. Prokes and A. Podlesnyak for their support with the neutron-diffraction measurements at BENSC. This research project has been supported in part by the European Commission under the 6th Framework Programme through the Key Action: Strengthening the European Research Area, Research Infrastructures, Contract No. RII3-CT-2003-505925 (NMI3). The work of A. A. Nugroho is supported by the NWO Breedtestrategie Program of the Zernike Institute for Advanced Materials, University of Groningen, and by KNAW, the Dutch Royal Academy of Sciences, through the SPIN program.

[1] S.-W. Cheong and M. Mostovoy, Nat. Mater. **6**, 23 (2007).
[2] T. Kimura, T. Goto, H. Shintani, K. Ishizaka, T. Arima, and Y. Tokura, Nature (London) **426**, 55 (2003).
[3] T. Kimura, G. Lawes, T. Goto, Y. Tokura, and A. P. Ramirez, Phys. Rev. B **71**, 224425 (2005).
[4] M. Kenzelmann, A. B. Harris, S. Jonas, C. Broholm, J. Schefer, S. B. Kim, C. L. Zhang, S.-W. Cheong, O. P. Vajk, and J. W. Lynn, Phys. Rev. Lett. **95**, 087206 (2005).
[5] M. Mostovoy, Phys. Rev. Lett. **96**, 067601 (2006).
[6] T. Goto, T. Kimura, G. Lawes, A. P. Ramirez, and Y. Tokura, Phys. Rev. Lett. **92**, 257201 (2004).
[7] R. Kajimoto, H. Yoshizawa, H. Shintani, T. Kimura, and Y. Tokura, Phys. Rev. B **70**, 012401 (2004).
[8] N. Abe, K. Taniguchi, S. Ohtani, T. Takenobu, Y. Iwasa, and T. Arima, Phys. Rev. Lett. **99**, 227206 (2007).
[9] H. Katsura, N. Nagaosa, and A. V. Balatsky, Phys. Rev. Lett. **95**, 057205 (2005).
[10] R. Feyerherm, E. Dudzik, N. Aliouane, and D. N. Argyriou, Phys. Rev. B **73**, 180401(R) (2006).
[11] G. A. Samara, J. Phys.: Condens. Matter **15**, R367 (2003).
[12] J. Blasco, C. Ritter, J. Garcia, J. M. de Teresa, J. Perez-Cacho, and M. R. Ibarra, Phys. Rev. B **62**, 5609 (2000).
[13] T. Kimura, S. Ishihara, H. Shintani, T. Arima, K. T. Takahashi, K. Ishizaka, and Y. Tokura, Phys. Rev. B **68**, 060403(R) (2003).
[14] D. Meier, N. Aliouane, D. N. Argyriou, J. A. Mydosh, and T. Lorenz, New J. Phys. **9**, 100 (2007).
[15] O. Peña, M. Bahout, D. Gutierrez, P. Duran, and C. Moure, Solid State Sci. **5**, 1217 (2003).
[16] J. A. Alonso, M. J. Martinez-lope, M. T. Casais, and M. T. Fernández-Diaz, Inorg. Chem. **39**, 917 (2000).
[17] J.-S. Zhou and J. B. Goodenough, Phys. Rev. B **68**, 144406 (2003).
[18] T. Mori, N. Kamegashira, K. Aoki, T. Shishido, and T. Fukuda, Mater. Lett. **54**, 238 (2002).
[19] D. Dabrowski, S. Kolesnik, A. Basszczuk, O. Chmaissem, T. Maxwell, and J. Mais, J. Solid State Chem. **178**, 629 (2005).
[20] R. D. Shannon and C. T. Prewitt, Acta Crystallogr., Sect. A: Cryst. Phys., Diffr., Theor. Gen. Crystallogr. **32**, 751 (1976).
[21] A. A. Bokov and Z.-G. Ye, J. Mater. Sci. **41**, 31 (2006).